

## **$^1\text{H}$ - $^1\text{H}$ Correlation via Isotropic Mixing of $^{13}\text{C}$ Magnetization, a New Three-Dimensional Approach for Assigning $^1\text{H}$ and $^{13}\text{C}$ Spectra of $^{13}\text{C}$ -Enriched Proteins**

AD BAX, G. MARIUS CLORE, AND ANGELA M. GRONENBORN

*Laboratory of Chemical Physics, National Institute of Diabetes and Digestive and Kidney Diseases,  
National Institutes of Health, Bethesda, Maryland 20892*

Received February 19, 1990

Recently, several new three-dimensional techniques for obtaining assignments of the amino acid side-chain resonances of larger proteins have been proposed (1-3). For these larger proteins (>10 kDa), conventional 2D NMR experiments such as COSY and HOHAHA/TOCSY yield spectra that typically exhibit extensive resonance overlap in the aliphatic region. Moreover, because for these slowly tumbling macromolecules the natural  $^1\text{H}$  linewidth ( $1/\pi T_2$ ) is often significantly larger than many of the  $^1\text{H}$ - $^1\text{H}$  couplings, the sensitivity of these homonuclear  $J$  correlation experiments is relatively low. Isotopic labeling with  $^{13}\text{C}$  results in a significant decrease in the proton transverse relaxation time,  $T_2$ , making homonuclear  $J$  correlation techniques even less sensitive. Therefore, separating the overlapping homonuclear  $^1\text{H}$  COSY or HOHAHA spectra in a 3D experiment according to the chemical-shift frequencies of attached  $^{13}\text{C}$  nuclei (4, 5) is inefficient for macromolecules.

The new techniques (1-3) do not rely on the poorly resolved  $^1\text{H}$ - $^1\text{H}$   $J$  couplings to establish  $J$  connectivity, but instead utilize the well-resolved one-bond  $^1\text{H}$ - $^{13}\text{C}$  and  $^{13}\text{C}$ - $^{13}\text{C}$   $J$  couplings to transfer magnetization. One approach, named 3D CCH-TOCSY-REVINEPT (1), starts with  $^{13}\text{C}$  magnetization which is transferred via isotropic mixing (6, 7) to other  $^{13}\text{C}$  spins within the same amino acid, followed by a reverse INEPT-type transfer (8, 9) to directly attached protons. The 3D version of this experiment yields  $^1\text{H}$ - $^{13}\text{C}$  shift correlation spectra that exhibit correlations between a proton and many of the  $^{13}\text{C}$  resonances in the same amino acid. These correlation spectra are separated into a third dimension according to the shift of the  $^{13}\text{C}$  directly attached to the observed  $^1\text{H}$ . An alternative approach, simply named HCCH (2, 3) or HCCH-COSY, starts with magnetization transfer from  $^1\text{H}$  to  $^{13}\text{C}$ . A subsequent COSY-type mixing transfers  $^{13}\text{C}$  magnetization to its  $^{13}\text{C}$  coupling partners which is followed by a reverse INEPT transfer to attached protons. The attractive features of this latter approach are the increased sensitivity (because the magnetization transfer process starts with  $^1\text{H}$ ) and the convenient presentation:  $^1\text{H}$ - $^1\text{H}$  correlation spectra separated in the third dimension according to the  $^{13}\text{C}$  shift.

Here we demonstrate a novel experiment that combines the advantages of the HCCH-COSY approach with the indirect connectivity information provided by the CCH-TOCSY-REVINEPT experiment. The pulse scheme for the new HCCH-

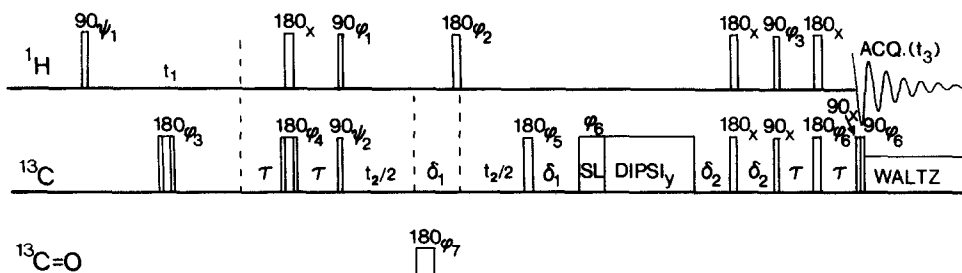


FIG. 1. Pulse scheme of the HCCH-TOCSY experiment. The delays  $\tau$  are set to  $1/(4J_{CH})$ , 1.5 ms in practice. The delays  $\delta_1$  and  $\delta_2$  are set to  $\sim 1/(6J_{CH})$ , 1.1 ms in practice, to permit net magnetization transfer to and from methine, methylene, and methyl resonances in the same experiment (20). The phase cycling is as follows:  $\phi_1 = y, -y$ ;  $\phi_2 = 4(x), 4(y), 4(-x), 4(-y)$ ;  $\phi_3 = 8(x), 8(-x)$ ;  $\phi_4 = 2(x), 2(-x)$ ;  $\phi_5 = 2(x), 2(y), 2(-x), 2(-y)$ ;  $\phi_6 = 4(x), 4(-x)$ ;  $\phi_7 = 8(x), 8(y)$ ; Acq. =  $2(x, -x, -x, x), 2(-x, x, x, -x)$ . The duration of the spin-lock trim pulse (SL), applied with phase  $\phi_6$ , is set to 2 ms. All the pulses of the DIPSI sequence are applied along the  $\pm y$  axis. The  $^{13}\text{C}$  carrier is positioned in the center of the aliphatic region of the spectrum ( $\sim 43$  ppm) and the carbonyl  $180^\circ_\phi$  pulse is applied as a DANTE series consisting of thirty-six  $5^\circ$  pulses having a duration of  $10 \mu\text{s}$  each, with the phase of each successive  $5^\circ$  pulse decremented by  $60^\circ$ . The  $180^\circ_\phi$  and  $180^\circ_\phi$  pulses are of the composite type  $(90^\circ_x 180^\circ_\phi 90^\circ_x)$ . Quadrature in the  $F_1$  and  $F_2$  dimensions is obtained with the TPPI-States method (21) using  $\psi_1 = 16(x), 16(y)$ ;  $\psi_2 = 32(x), 32(y)$ . Each time  $t_1$  is incremented, the receiver reference phase and  $\psi_1$  are also incremented by  $180^\circ$ . Each time  $t_2$  is incremented, the receiver phase and  $\psi_2$  are also incremented by  $180^\circ$ . Data obtained for  $\psi_1 = x$ ,  $y$  and  $\psi_2 = x, y$  are stored separately and processed as complex data.

TOCSY experiment is sketched in Fig. 1. The scheme is very similar to the previously described HCCH-COSY experiment, with the main difference that the  $90^\circ$   $^{13}\text{C}$  COSY mixing pulse now has been replaced by an isotropic mixing scheme of the DIPSI type (10). Briefly, the pulse scheme functions as follows. After the evolution period,  $t_1$ ,  $^1\text{H}$  magnetization is transferred to  $^{13}\text{C}$  in an INEPT-type manner. The antiphase  $^{13}\text{C}$  magnetization is refocused during the intervals  $\delta_1$  ( $\sim 1$  ms each), and the  $^{13}\text{C}$  magnetization evolves during the second evolution period,  $t_2$ , under influence of the  $^{13}\text{C}$  chemical shift. The  $180^\circ_{\phi_2}$  pulse removes the net effect of  $^1\text{H}$ - $^{13}\text{C}$  coupling during the  $t_2$  period, and a low-power  $180^\circ$  pulse applied to the carbonyl ( $\text{C}'$ ) resonances eliminates  $J_{\text{C}\alpha\text{C}'}$  dephasing of the  $\text{C}\alpha$  magnetization. At the end of the  $t_2$  evolution period, a short "trim pulse" applied along the  $x$  axis defocuses all in-phase  $^{13}\text{C}$  magnetization that is not parallel to the effective field. The subsequent DIPSI isotropic mixing scheme transfers the remaining net  $^{13}\text{C}$  magnetization to its neighbors. Finally, a reverse INEPT sequence converts this  $^{13}\text{C}$  magnetization back to the attached protons, which are detected during  $t_3$ .

The main technical difficulty of this experiment is posed by the requirement to obtain isotropic mixing of the  $^{13}\text{C}$  spins. The spectral width of  $^{13}\text{C}$  is considerably larger than that of  $^1\text{H}$ , and it is therefore more difficult to achieve efficient isotropic mixing. Commonly used mixing schemes such as MLEV-17 (7) or WALTZ-17 are derivatives of heteronuclear decoupling schemes and are not optimized for the purpose of isotropic mixing (11). As demonstrated by Waugh (12), such a mixing sequence applied to two coupled spins,  $I_1$  and  $I_2$ , results in a multitude of undesired terms in the average Hamiltonian, including cross products of the form  $J I_{1\alpha} I_{2\beta}$ , with a  $\alpha, \beta = x, y, z$  and  $\alpha \neq \beta$ , and linear terms  $I_{1\alpha}$  and  $I_{2\alpha}$ . These undesirable terms

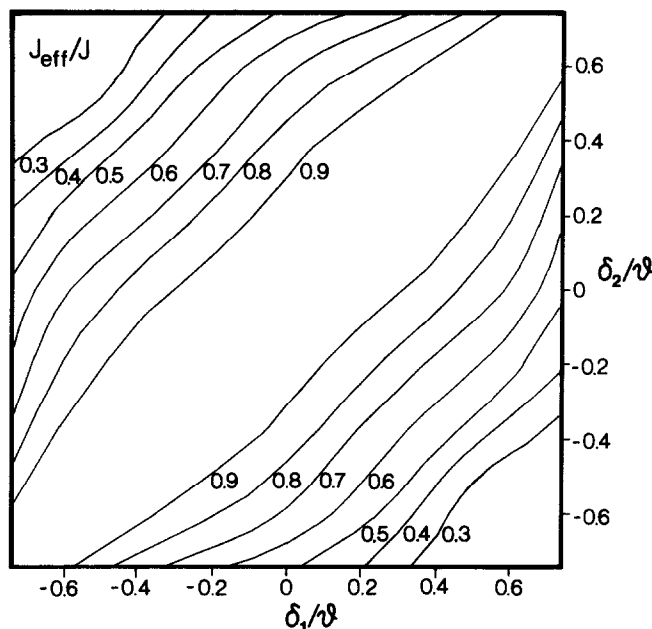


FIG. 2. Scaling of the effective  $J$  coupling constant during application of a DIPSI-3 mixing scheme, as a function of the resonance offsets,  $\delta_1$  and  $\delta_2$ , of the two spins, divided by the strength of the applied RF field. For the relatively large one-bond  $J_{CC}$  couplings, the approximation that DIPSI-3 produces a pure scalar operator is valid in the region of the diagram for which  $J_{\text{eff}} > 0.5J$ .

interfere with the isotropic mixing process and as Shaka *et al.* (10) pointed out, they also have a negative effect on heteronuclear spin decoupling in the presence of homonuclear interactions.

New composite pulse decoupling schemes developed by Shaka *et al.* have been optimized to yield an effective Hamiltonian during mixing that minimizes the magnitude of the undesirable terms, resulting in an average Hamiltonian that contains only a scalar interaction,  $J_{\text{eff}} \mathbf{I}_1 \cdot \mathbf{I}_2$ . As pointed out by Rucker and Shaka (13) and Titman *et al.* (14), these so-called DIPSI sequences are therefore also very effective for homonuclear isotropic mixing. For the case of  $^{13}\text{C}$ , computer simulations indicate that the DIPSI-3 sequence (10) yields the largest isotropic mixing bandwidth for a given amount of RF power. For the case of  $^{13}\text{C}$ , with  $J_{CC} \approx 35$  Hz, an RF field strength of  $\nu$  hertz provides effective isotropic mixing over a bandwidth of about  $\pm 0.75\nu$ . However, for coupled spins that have significantly different offsets, the effective  $J$  coupling during isotropic mixing,  $J_{\text{eff}}$ , can become significantly smaller than the real  $J$  coupling, resulting in a slowdown of the isotropic mixing process. If the angle between the effective fields experienced by two coupled spins equals  $\theta$  and  $\theta \ll \pi/2$ , the reduction in  $J$  coupling is approximately given by (10)

$$J_{\text{eff}} \approx J[1 - (1 - \cos \theta)\sqrt{8/3}]. \quad [1]$$

Figure 2 shows this decrease in the effective coupling constant as a function of the resonance offsets of the two spins,  $\delta_1$  and  $\delta_2$ . This figure results from a computer

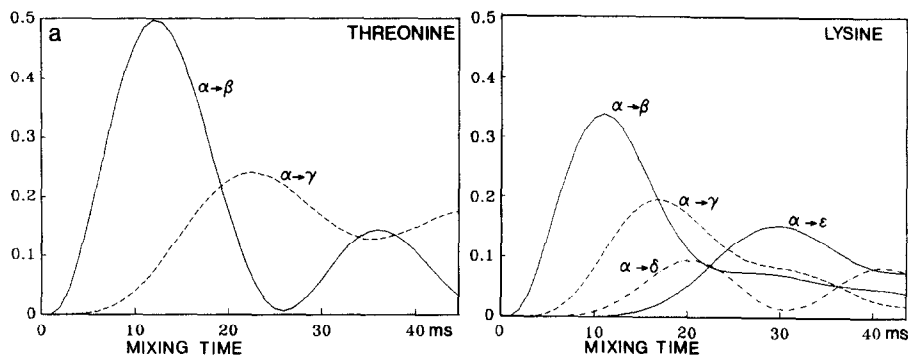


FIG. 3. The fraction of  $^{13}\text{C}$  magnetization transferred to side-chain carbons during ideal isotropic mixing for (a) threonine and (b) lysine. For threonine, the reduced effective  $J$  couplings used for calculating the graphs are  $J_{C\alpha C\beta} = 35$  Hz and  $J_{C\beta C\gamma} = 19$  Hz. For lysine, all one-bond  $J$  couplings are assumed to be 33 Hz. For both spin systems, multiple-bond carbon-carbon couplings are neglected.

simulation of the DIPSI-3 sequence and shows a behavior that is qualitatively predicted by Eq. [1].

Even with the DIPSI-type mixing schemes it does not appear feasible to extend the isotropic mixing over the entire  $^{13}\text{C}$  bandwidth on high-field spectrometers. However, for proteins, coverage of the aliphatic region (10–70 ppm) alone is sufficient for most practical purposes. On a 500 MHz spectrometer this requires a minimum  $^{13}\text{C}$  RF field of about 5 kHz, which can be easily obtained with relatively low power on regular inverse probeheads, optimized for  $^1\text{H}$  detection. As discussed below, to limit the reduction in  $J$  coupling, a somewhat stronger RF field is desirable.

The largest chemical-shift difference for directly attached aliphatic carbons is found in threonine residues, where the  $C\beta$  and  $C\gamma$  carbons differ in chemical shift by about 50 ppm. Because of this large chemical-shift difference, the effective  $J$  coupling is significantly smaller than the real  $C\beta$ – $C\gamma$  coupling (38 Hz). Figure 2 indicates that in order to ensure that  $J_{\text{eff}} > J_{C\beta C\gamma}/2$ , it is necessary that the RF field strength,  $\nu$ , is larger than  $\sim(\delta_1 - \delta_2)/0.85$ . Hence, on a 500 MHz spectrometer, an  $\sim 7$  kHz RF field is needed to limit the reduction in effective  $J$  coupling to less than 50%. For all other amino acids, the reduction in  $J$  coupling is much less severe. For example, for the next most difficult amino acid, alanine, the  $C\alpha$  and  $C\beta$  shifts differ by about 35 ppm and  $J_{\text{eff}}$  is reduced by about 35% when using a 7 kHz RF field on a 500 MHz spectrometer. All other  $J$  couplings are reduced by amounts that are significantly smaller than 35%.

To a first approximation, the magnetization transfer along a chain of coupled  $^{13}\text{C}$  nuclei can be simulated assuming ideal isotropic mixing in the presence of the reduced  $J$  couplings,  $J_{\text{eff}}$ . Two- and three-bond aliphatic carbon-carbon couplings are small and may safely be neglected. Figure 3 shows the net  $^{13}\text{C}$  magnetization transfer from the  $C\alpha$  nucleus to the side-chain spins as a function of mixing period duration for the amino acids threonine and lysine. Relaxation during the isotropic mixing occurs at a rate that is on the order of the  $^{13}\text{C}$  transverse relaxation rate,  $1/T_2$ . For the simulations shown in Fig. 3, a  $T_2$  of 30 ms has been assumed.

The HCCH-TOCSY technique of Fig. 1 is demonstrated for a 1.8 mM sample of the protein interleukin-1 $\beta$  (156 residues, 17 kDa) dissolved in  $\text{D}_2\text{O}$ , p $^2\text{H}$  5.2, 35°C.

Spectra were recorded on a Bruker AM-500 spectrometer that has been modified to eliminate overhead time at the end of every  $t_1$  and  $t_2$  increment. The  $^1\text{H}$  carrier was positioned at 3.0 ppm, and the  $^{13}\text{C}$  carrier at 43 ppm. All proton pulses were applied with a 10 kHz RF field.  $^{13}\text{C}$  pulses were applied using a 7 kHz RF field ( $\sim 12.5$  W RF power), and the DANTE-type carbonyl inversion pulse (3) was applied with a weak 1.4 kHz RF field. Three loops of the DIPSI-3 sequence were used for isotropic mixing, corresponding to a duration of 24 ms. For  $^{13}\text{C}$  decoupling during data acquisition, the  $^{13}\text{C}$  power was reduced to 3.1 W. Acquisition times were 34, 12, and 51 ms in the  $t_1$ ,  $t_2$ , and  $t_3$  dimension, respectively. The size of the acquired 3D matrix was (128 complex)  $\times$  (32 complex)  $\times$  (512 real). Using a delay time of 0.9 s between scans, the total measuring time was 70 h. 3D data were processed with a combination of commercial software (NMRi, Syracuse, New York) and home-written programs for Fourier transformation in the third dimension (15). Fifty degree phase-shifted sine-bell filtering and zero filling were used in all three dimensions. As previously described for the HCCH-COSY experiment (3), delay durations are adjusted such that no phase correction is required in the  $F_1$  and  $F_2$  dimensions of the final 3D spectrum.

Figure 4 shows two slices taken from the 3D HCCH-TOCSY spectrum of interleukin- $\beta$ . These slices contain the same kind of information as a regular 2D HOHAHA spectrum, but spectral overlap is reduced tremendously. The shift of the  $^{13}\text{C}$  attached to the proton on the diagonal determines the  $F_2$  coordinate in the 3D spectrum. The multiple folding used in the  $^{13}\text{C}$  dimension does not constitute any problem since the  $^1\text{H}$  chemical shift of the diagonal peak and the pattern of cross peaks observed for such a peak usually identify the correct  $^{13}\text{C}$  chemical shift. For example, in Fig. 4B the diagonal peaks between 5.5 and 3.5 ppm all show cross peaks to resonances further upfield, indicating that they correspond to  $\text{H}\alpha$  resonances, and that the 58.98 ppm  $^{13}\text{C}$  shift applies. Similarly, cross-peak patterns observed for diagonal resonances near 1 ppm indicate that these resonances correspond to methyl groups of valine and alanine residues, and that the 17.56 ppm shift (and not 38.27 or 58.98 ppm) applies to these resonances.

The cross-peak intensities in the 3D spectrum largely follow the predicted patterns. For example, for Thr-9 in Fig. 4B the  $\text{H}\alpha$ - $\text{H}\beta$  cross peak is too weak to be observed, but the  $\text{H}\alpha$  to  $\text{C}\gamma\text{H}_3$  cross peak is intense as predicted in Fig. 3a. For lysine residues, the cross peaks between  $\text{H}\alpha$  and  $\text{H}\beta$  and  $\text{H}\gamma$  protons are expected to be more intense than the cross peaks to  $\text{H}\delta$  and  $\text{H}\epsilon$  protons (Fig. 3b), whereas Fig. 4B indicates that the  $\text{H}\alpha/\text{H}\epsilon$  cross peak has the highest intensity. This qualitative discrepancy is most likely caused by the increased mobility at the end of the long lysine side chains, which increases the efficiency of the last reverse INEPT transfer and narrows the  $^1\text{H}$   $F_3$  linewidth. It should also be noted that cross peaks to the magnetically equivalent  $\text{H}\epsilon$  protons superimpose the intensity of both methylene protons, doubling their resonance intensity relative to the case of nonequivalent methylene protons. The net magnetization transfer as depicted in Fig. 3 does not take into account the effect of  $J_{\text{CC}}$  dephasing during the periods  $t_1$ ,  $\delta_1$ , and  $\delta_2$ , which has the tendency to shift the curves shown in Fig. 3 to the left by several milliseconds.

Two protons with chemical shifts HA and HB, attached to two  $J$ -coupled carbons CA and CB, show an  $(F_1, F_3) = (\text{HA}, \text{HB})$  cross peak in a slice taken at  $F_2 = \text{CA}$ .

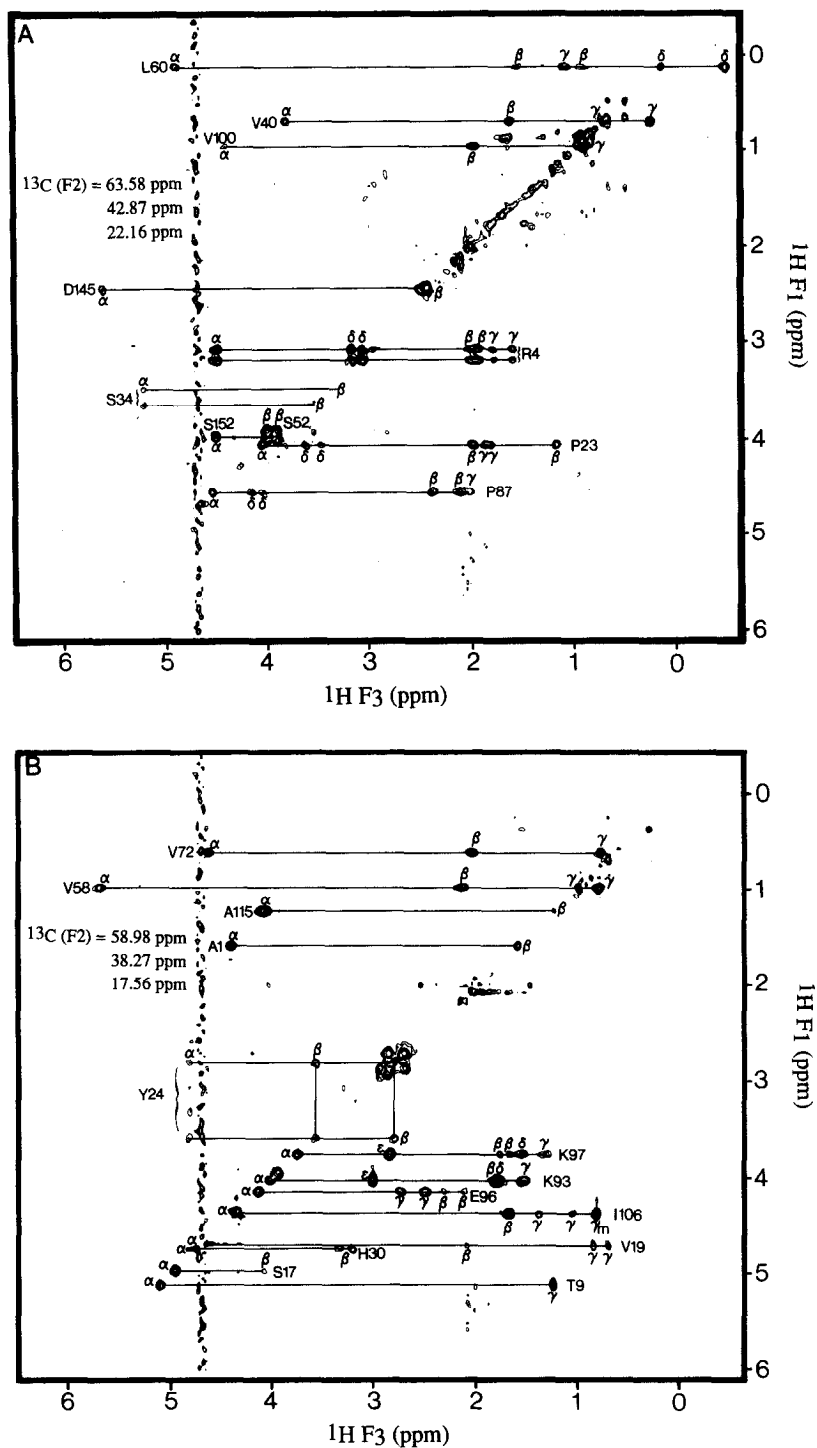


FIG. 4. Two out of 64 ( $F_1$ ,  $F_3$ ) slices of the 3D HCCH-TOCSY spectrum of a 1.8 mM solution of interleukin-1 $\beta$  in  $\text{D}_2\text{O}$ , recorded at 500 MHz, using a 24 ms mixing period and a 2 ms trim pulse. Because the  $F_2$  spectral width was set to 20.71 ppm, extensive folding occurs in this dimension and each slice contains resonances corresponding to three different  $^{13}\text{C}$  chemical shifts. The 3D spectrum results from a (128 complex)  $\times$  (32 complex)  $\times$  (512 real) data matrix, and the total measuring time was 70 h.

The mirror-image cross peak at  $(F_1, F_3) = (\text{HB}, \text{HA})$  is present in a slice taken at  $F_2 = \text{CB}$ . The fact that every cross peak has such a mirror image allows one to determine both  $^1\text{H}$  and  $^{13}\text{C}$  shifts for all cross peaks. Combined analysis of the 3D HCCH-TOCSY spectrum and the previously described HCCH-COSY spectrum together with a triple-resonance 3D HNCA spectrum that correlates NH,  $^{15}\text{N}$ , and  $\text{C}\alpha$  chemical shifts (16, 17) provided sufficient information to make complete  $^1\text{H}$  and  $^{13}\text{C}$  assignments of interleukin-1 $\beta$ . With this information in hand, analysis of the 3D NOESY-HMQC spectrum (18, 19) of this protein is quite straightforward, making structure determination of proteins the size of interleukin-1 $\beta$  a feasible task.

## ACKNOWLEDGMENTS

We thank Paul Wingfield for the sample of uniformly  $^{15}\text{N}$ - and  $^{13}\text{C}$ -labeled interleukin-1 $\beta$  and Rolf Tschudin for technical assistance. The computer simulations for Figs. 2 and 3 were performed with the program ANTIOPE, kindly provided by Technic de Bouregas. This work was supported by the Intramural AIDS Antiviral Program of the Office of the Director of the National Institutes of Health.

## REFERENCES

1. S. W. FESIK, H. L. EATON, E. T. OLEJNICZAK, E. R. P. ZUIDERWEG, L. P. MCINTOSH, AND F. W. DAHLQUIST, *J. Am. Chem. Soc.* **112**, 886 (1990).
2. L. E. KAY, M. IKURA, AND A. BAX, *J. Am. Chem. Soc.* **112**, 888 (1990).
3. A. BAX, G. M. CLORE, P. C. DRISCOLL, A. M. GRONENBORN, M. IKURA, AND L. E. KAY, *J. Magn. Reson.*, in press.
4. S. W. FESIK, R. T. GAMPE, AND E. R. P. ZUIDERWEG, *J. Am. Chem. Soc.* **111**, 770 (1989).
5. S. S. WIJMEGA, K. HALLENGA, AND C. W. HILBERS, *J. Magn. Reson.* **84**, 634 (1989).
6. L. BRAUNSCHWEILER AND R. R. ERNST, *J. Magn. Reson.* **53**, 521 (1983).
7. A. BAX AND D. G. DAVIS, *J. Magn. Reson.* **65**, 355 (1985).
8. R. FREEMAN, T. H. MARECI, AND G. A. MORRIS, *J. Magn. Reson.* **42**, 341 (1981).
9. M. R. BENDALL, D. T. PEGG, AND D. M. DODDRELL, *J. Magn. Reson.* **45**, 8 (1981).
10. A. J. SHAKA, C. J. LEE, AND A. PINES, *J. Magn. Reson.* **77**, 274 (1988).
11. A. BAX, *Isr. J. Chem.* **28**, 309 (1988).
12. J. S. WAUGH, *J. Magn. Reson.* **68**, 189 (1986).
13. S. P. RUCKER AND A. J. SHAKA, *Mol. Phys.* **68**, 509 (1989).
14. J. TITMAN, D. NEUHAUS, AND J. KEELER, *J. Magn. Reson.* **85**, 111 (1989).
15. L. E. KAY, D. MARION, AND A. BAX, *J. Magn. Reson.* **84**, 72 (1989).
16. M. IKURA, L. E. KAY, AND A. BAX, *Biochemistry*, in press.
17. L. E. KAY, M. IKURA, R. TSCHUDIN, AND A. BAX, *J. Magn. Reson.*, in press.
18. M. IKURA, L. E. KAY, AND A. BAX, *J. Magn. Reson.* **86**, 204 (1990).
19. E. R. P. ZUIDERWEG, L. P. MCINTOSH, F. W. DAHLQUIST, AND S. W. FESIK, *J. Magn. Reson.* **86**, 210 (1990).
20. D. P. BURUM AND R. R. ERNST, *J. Magn. Reson.* **39**, 163 (1980).
21. D. MARION, M. IKURA, R. TSCHUDIN, AND A. BAX, *J. Magn. Reson.* **85**, 393 (1989).